

## **SHEAR BEHAVIOR OF 45-YEAR-OLD AASHTO TYPE II BRIDGE GIRDERS**

**Cameron D. Murray**, University of Oklahoma, Norman, OK  
**Brittany N. Cranor**, Guernsey Engineers, Architects, and Consultants, Oklahoma City, OK  
**Royce W. Floyd, Ph.D., P.E.**, University of Oklahoma, Norman, OK  
**Jin-Song Pei, Ph.D.**, University of Oklahoma, Norman, OK

### **ABSTRACT**

*A number of bridges in the state of Oklahoma designed under previous versions of the AASHTO Standard Specifications have the potential to be inadequate for shear when compared to the current AASHTO LRFD Specifications due to differences in how the demand side of the shear strength equation is calculated. Two approximately 45-year-old AASHTO Type II bridge girders taken from the I-244 bridge over the Arkansas River in Tulsa, Oklahoma, were subjected to a series of non-destructive flexural tests and final destructive shear tests in order to assess behavior characteristics of aged prestressed members. The nondestructive flexural tests were used to estimate the flexural stiffness and effective prestress force and the girders were tested with two different sections of the bridge deck and diaphragms intact to examine the contribution of the deck to capacity. Shear capacity was predicted based on the original design specifications, the current AASHTO LRFD Specifications, and methods proposed by other researchers. Measured capacity exceeded the predicted values in all cases, but deterioration near the girder ends was observed to influence the failure mechanisms.*

**Keywords:** Shear, Bridge Girders, Bond

## INTRODUCTION

In 2013, two bridge girders were selected from separate spans of the eastbound side of the I-244 bridge over the Arkansas River in Tulsa, OK for testing at the Fears Structural Engineering Laboratory at the University of Oklahoma (OU). The bridge was constructed in the late 1960's and its demolition in 2013 provided a rare opportunity to test girders that were in service for decades. The ends of the girders included some corrosion damage that is typical of urban bridges in Oklahoma and may be cause for concern regarding the shear capacity of the girders. The Oklahoma Department of Transportation (ODOT) is interested in the shear capacity of older bridge girders because of the deterioration of the end regions and because these girders were designed under an older version of the American Association of State Highway and Transportation Officials (AASHTO) bridge code. The bridge code at the time assumed a different critical section for shear than what is used today and also provided a different method of calculating shear capacity. The design demands from the previous code and the deterioration over time combine to create potential low ratings for shear using the current methods. It is possible that the older designs are not only less conservative for shear, but the presence of corrosion could reduce the bond of prestressing strands near the member ends. In addition to the specific concerns of ODOT, there are few studies of bridge girders at the end of their service life, and even fewer that considered shear capacity specifically.

This paper contains preliminary results from the research including a comparison of tested capacities from both ends of the two bridge girders to AASHTO codes and the American Concrete Institute (ACI) code.<sup>1,2,3</sup> This work is focused on comparing the results of shear tests on Type-II girders to code equations. No literature was found documenting shear performance of aged Type-II girders, so this paper adds to the body of knowledge on shear. Issues of corrosion of the girder ends were also examined as they relate to the performance of the beam up to the quarter span point. The information gained from the testing described is intended to inform rating decisions for bridges constructed with similar girder designs and deterioration.

## BACKGROUND

The end regions of concrete members are of particular importance to the designer of a prestressed concrete girder for several reasons. The ends are where the largest shear forces are present, where prestress force is transferred to the concrete, where the largest stresses due to prestress release are located if no harping or strand debonding is utilized, and where corrosion is most likely to occur. Corrosion at this location is common because joints between simply supported spans tend to leak water and deicing chemicals on the ends of the girders. Even though the stress at the extreme end is zero, the "end" of the girder in this paper refers to the first quarter of the span (because this was the critical section for shear at the time these girders were designed), so the transfer length is included in this section. While the presence of a prestress force improves the shear capacity of a section, strand bond can be lost when shear cracking occurs.<sup>4,5</sup> If bond is lost, the capacity of the member is significantly

diminished. Early research at the University of Illinois found that transverse reinforcement restrains shear cracking and improves ductility after web cracks form.<sup>6</sup> These findings led to equations for the shear capacity of concrete and minimum shear reinforcement.<sup>7</sup> The shear methodology in the ACI Building Code Requirements for Structural Concrete<sup>3</sup> were developed based on this early work and the equations remain largely unchanged.

### ACI SHEAR PROVISIONS

The ACI treatment of shear in prestressed concrete is given in Chapters 9 and 22 of the 2014 code and involves a separate calculation of the contribution of the steel and the concrete to the shear resistance.<sup>3</sup> The nominal shear capacity of a section is given by Equation 1.

Equation 1

where:

- $V_n$  = Nominal shear capacity (lb)
- $V_c$  = Concrete contribution to shear strength (lb)
- $V_s$  = Steel contribution to shear strength (lb)

For prestressed concrete members, the ACI code offers two methods to calculate shear capacity of the concrete: a simplified method and a more complex method that takes into account different cracking behavior and failure mechanisms. The complex method provides an equation for web-shear cracking and flexure-shear cracking to find the controlling type of cracking at a given section. For this research, the minimum of the capacity given by the two methods was chosen. The simplified method is given in Equation 2.

Equation 2

where:

and:

- $\lambda$  = Modification factor for lightweight aggregate; 1.0 for normal weight
- $f'_c$  = Specified compressive strength of concrete (psi)
- $V_u$  = Factored applied shear at section (lb)
- $d_p$  = Depth to centroid of prestress force from extreme compression fiber (in.)
- $M_u$  = Factored moment at section (in.-lb)
- $b_w$  = Width of web (in.)
- $d$  = Distance from extreme compression fiber to centroid of tensile reinforcement (in.)

For the more complex method in ACI, the concrete contribution related to flexure-shear capacity is given by Equation 3.

Equation 3

where:

and:

$V_{ci}$  = Nominal shear strength provided by concrete when diagonal cracking results from combined shear and moment (lb)

$V_d$  = Shear force at section due to unfactored dead load (lb)

$V_i$  = Factored shear force at section due to externally applied loads associated with  $M_{max}$  (lb)

$M_{cre}$  = Moment causing flexural cracking at section due to external loads (in.-lb)

$M_{max}$  = Maximum factored moment due to external loads (in.-lb)

$y_t$  = Distance from centroid of gross section to tension face (in.)

$I$  = Moment of inertia of cross-section (in<sup>4</sup>)

$f_{pe}$  = Stress in concrete due to effective prestress force at tension face (psi)

$f_d$  = Stress due to unfactored dead load at tension face (psi)

The nominal shear force required to cause web-shear cracking is given by Equation 4.

Equation 4

where:

and:

$V_{cw}$  = Nominal shear strength provided by concrete when diagonal cracking results from high principal tensile stress in web (lb)

$f_{pc}$  = Compressive stress in concrete after losses at centroid of the section resisting external loads or at the junction of the web and the flange when the centroid is within the flange (psi)

$V_p$  = Vertical component of effective prestress force at section (psi)

The shear strength supplied by the transverse reinforcement is given by Equation 5. For vertical shear stirrups, the ACI code assumes a crack angle of 45 degrees. This approach likely overestimates the angle of shear cracking for prestressed beams but will give a conservative value for the steel contribution to shear strength.

Equation 5

where:

$A_v$  = Area of shear reinforcement within spacing,  $s$  (in<sup>2</sup>)

$$\begin{aligned}
 f_{yt} &= \text{Yield strength of transverse reinforcement (psi)} \\
 s &= \text{Spacing of shear reinforcement at section (in.)}
 \end{aligned}$$

The ACI methodology has not changed since the 1970's. ACI also allows the use of a strut-and-tie model for analysis and design in discontinuity regions of concrete beams.

## AASHTO STANDARD SPECIFICATIONS SHEAR DESIGN

The AASHTO shear philosophy has evolved considerably since the 1970's. At that time, the governing bridge code was the AASHTO Standard Specifications for Highway Bridges (from here on referred to as AASHTO-STD). This code used a load factor design (LFD) philosophy for concrete. One concern regarding bridge girders designed at this time is the location of the critical section for shear. The code at this time recommended investigating shear only in the middle half of the span. The reasoning was that the critical section for shear would be at a location where shear and flexural forces interact. At locations closer to the support than the "quarter-point" the shear demand was to be taken the same as at the quarter-point. It is possible that higher shear demands at the ends could lead to a lack of conservatism for these older designs.

Nominal shear strength is determined in a similar fashion to ACI in AASHTO-STD; by summing the contributions of the steel and the concrete. The shear resistance in AASHTO-STD in 1973 is given by Equation 6.<sup>1</sup>

Equation 6

where:

$$\begin{aligned}
 b' &= \text{Width of web (in.)} \\
 j &= \text{Ratio of distance between centroid of compression and centroid of} \\
 &\quad \text{tension and total depth} \\
 f_{sy} &= \text{Tensile capacity of shear reinforcement (psi)}
 \end{aligned}$$

This procedure is quite similar to the ACI method, although it is more simplistic with regards to the contribution of concrete to shear strength. As for the steel contribution to shear strength, the "2" in the numerator of the second term in Equation 6 would correspond to a crack angle of 26.6 degrees, as opposed to 45 degrees in the ACI code. A smaller crack angle makes sense because prestress forces are known to flatten stress trajectories in girders,<sup>8</sup> however if the actual crack angle is greater than 26.6 degrees the steel capacity will be overestimated. A minimum shear steel requirement is given by Equation 7.

Equation 7

There is no upper limit on shear reinforcement in AASHTO-STD. However, the concrete contribution to shear strength is constrained by an upper limit on compressive strength of 3000 psi. A positive result of this requirement is that most girders designed at this time

required a larger amount of shear steel, despite the demand being taken further into the section. This conservatism with regards to concrete strength could improve the ductility of girders loaded in shear from this time period.

## AASHTO LOAD AND RESISTANCE FACTOR DESIGN

The AASHTO bridge code has also changed considerably overall since the 1970's. The current code now uses a probabilistic Load and Resistance Factor Design (LRFD) design philosophy.<sup>2</sup> For the rest of this paper, the current code (2012 version) will be referred to as AASHTO-LRFD. AASHTO-LRFD began using a new shear design methodology in 1994 known as the "sectional design model" based on Modified Compression Field Theory (MCFT).<sup>9,10,11</sup> This method was rather complex and was not preferred by designers as it required an iterative solution. This procedure was simplified in 2008 and there are now multiple options to calculate concrete shear capacity in the 2012 AASHTO-LRFD. The AASHTO-LRFD "simplified procedure" is similar to the ACI method because it divides a member into sections controlled by flexure-shear and web-shear.<sup>11</sup> Shear resistance is taken as the sum of the concrete shear strength, steel contribution to shear strength, and a term to account for the influence of prestress force on shear strength. Concrete contribution to shear strength is taken as the lesser of the resistance when cracking is caused by combined shear and moment or the resistance when cracking occurs in the web due to shear only (Equations 8, 9, and 10).

Equation 8

Equation 9

Equation 10

where:

$b_v$  = Effective web width taken as the minimum web width within  $d_v$  (in.)

$d_v$  = Effective shear depth taken as the distance between the resultant tensile and compressive forces due to flexure (in.)

The general method provided by AASHTO-LRFD is based on MCFT. MCFT assumes that a series of shear cracks will form in the web of a member, creating a network of diagonal concrete shear struts (in compression) and vertical steel stirrups (in tension) that work together to carry the total shear demand. Each concrete strut also carries some tension and the sum of the tension in all the struts is the concrete's contribution to the shear strength. In order to find shear resistance by MCFT, the factors  $\beta$  and  $\theta$  must be determined. The factor  $\beta$  describes the ability of the concrete to transmit tension and shear and  $\theta$  is the crack angle (or angle of diagonal compressive stress). In the original MCFT procedure, a series of tables were used to relate strains to  $\beta$  and  $\theta$ . In the current AASHTO-LRFD "general method" there are two equations used to estimate these factors, the  $\beta$  calculation is shown in Equation 11.

$$\text{If } A_v \geq \text{Minimum } A_v, \quad \text{Equation 11}$$

else,

where:

$\epsilon_s$  = Net longitudinal tensile strain at the centroid of the tension reinforcement

$s_{xe}$  = A spacing factor given in the code

The crack angle,  $\theta$ , can be found by the relationship in Equation 12.

Equation 12

This new procedure based on equations instead of tables was developed by Bentz et al.<sup>12</sup> in 2006 to simplify the MCFT procedure. If the minimum amount of shear steel is not provided, the equation for  $\beta$  assumes no transverse reinforcement. These simplified calculations should be conservative for almost all combinations of  $\beta$  and  $\theta$  as compared to the original tabular method. Today, the tables are maintained in AASHTO-LRFD as an appendix and are still allowed for design. The concrete contribution to shear strength is then given as a function of  $\beta$  by .

Finally, the steel contribution in AASHTO-LRFD is generally a function of the crack angle, rebar spacing, depth, stirrup angle, area, and yield strength of the reinforcement. This relationship is given in Equation 14.

Equation 14

where:

$\alpha$  = angle of inclination of transverse reinforcement

MCFT was introduced as a comprehensive, rational method for analyzing concrete members subjected to shear. Despite its more complicated nature, it should provide more accurate results than the ACI method and the AASHTO-STD method. It is hard to say definitively what effect older codes have on the conservatism of old designs because there are many variables involved in terms of demand and capacity. Because of the complex nature of these problems it is important to have experimental data from old girders for comparison to design codes.

## STRUT-AND-TIE MODELS

Another option allowed by both ACI and AASHTO-LRFD is the strut-and-tie model (STM). At regions near discontinuities (e.g. loads, supports, cross section changes), St. Venant's Principle is no longer an accurate assumption.<sup>13</sup> At these locations, Bernoulli beam theory does not provide accurate results for the shear capacity because the strain distribution is not linear. The STM was developed in the late 1800's to solve these types of problems.<sup>14</sup> STM creates a truss analogy where diagonally cracked concrete forms compressive "struts," and the longitudinal and transverse reinforcement form tension "ties." The STM does not provide a unique solution like the sectional methods, but will give a lower bound shear strength. STM has been used to verify details in concrete members but can be difficult to apply.<sup>11</sup> A STM will be considered for all the girders tested in this project at a later time.

## PREVIOUS WORK ON SHEAR IN AGED GIRDERS

There have been few studies that looked specifically at the shear capacity of older concrete girders. A number of studies have been conducted to test aged prestressed concrete girders for residual prestress or flexural strength,<sup>15-19</sup> but few have focused specifically on shear capacity.

Several studies were performed at the University of Florida on large scale sections in shear. In these studies, the researchers focused on varying the shear span to depth ( $a/d$ ) ratio, which alters the interaction between bending and shear stresses. These studies found that for  $a/d$  ratios of 3 or less, bond shear failures are common. When  $a/d$  is approximately equal to 4, compression or shear-compression failures occurred. Finally, at  $a/d$  of 5 or greater the failure mechanism transitioned to flexure. This work also found the ACI and MCFT methods to be conservative for  $a/d$  of 3 or less.<sup>20,21</sup>

At the University of Utah, seven 42-year-old girders were recovered for shear tests. These tests were performed at an  $a/d$  ratio of 1.5 using a single point load. Code equations were found to be conservative and STM was more accurate given that the load was near the support.<sup>22</sup>

Prior work at the University of Oklahoma (OU) was conducted in 2008 when researchers tested a 40-year-old AASHTO Type II girder in the lab to compare the 1973 and 2004 AASHTO codes. This girder was tested at  $a/d$  of 1.0 and the researchers found that all codes were conservative at this location.<sup>23</sup> The study reported here is a continuation of this work for ODOT, testing larger  $a/d$  ratios. The girder in this older study was damaged and the deck had been completely removed, so the current study expands the work to girders in better condition with partial deck and diaphragms remaining.

## DESCRIPTION OF TESTING

Two girders taken from the I-244 bridge over the Arkansas river in Tulsa, Oklahoma, were tested as part of this program. The first, girder "A," was a 32-ft-long AASHTO Type II

girder prestressed with six straight  $\frac{1}{2}$  in. strands and four harped strands. This girder had been cut from the full bridge in a way that left a section of the 8.5 in. deck of a roughly equal width to the top flange intact. More detail about girder A can be found in the master's thesis of one of the authors.<sup>24</sup> The second girder is labeled as girder "C" in this study, and it was taken from a different span of the same bridge. Girder C was a 46-ft-long AASHTO Type II girder prestressed with ten straight strands and six harped strands. It was delivered with a roughly 36 in. wide portion of deck. The deck was cut off-center however, so an additional 10 in. of deck was cast on the short side to regain section symmetry using a concrete mixture designed to match the strength of cores taken from the deck. Continuity was maintained by embedding number 4 bars in the existing girder using structural epoxy to the depths specified by the epoxy manufacturer. The spacing was selected based on the spacing of steel in the bridge deck and on interface shear forces using AASHTO 5.8.4. The concrete face was roughened with a jackhammer to improve the bond between the old and new deck concrete and meet the roughened surface requirements described in AASHTO 5.8.4.3. Girder C also had partial diaphragms remaining at the center and the ends. Both girders were reinforced for shear with double No. 4 Z bars spaced at 4 in. for the first 12 in. of the beam from each end, 8 in. until 30% of the length from each end, and 12 in. for the interior 40% of the beam. Figure 1 shows the girders prior to testing. Figure 2 and Figure 3 show the cross sections of the girders and the sections including the deck, respectively. The deck of both girders included a 2 in. concrete wearing overlay. This overlay tended to control the ability of the deck to carry compression forces.



Figure 1: Girders A (left) and C (right)

In order to evaluate the residual stiffness of "A," 17 elastic flexural tests up to a load of 15 kips were performed at varying load points and support locations. Deflection was measured along the length of the beam using linear variable differential transformers (LVDTs) centered on the girder soffit for all locations except the centerline where LVDTs were placed on each side of the bottom flange of the girder. Tensile strain due to bending was measured using strain gauges attached to the bottom flange. The cracking load from the shear tests was also used to estimate prestress force.

To continue the work of Martin et al.<sup>23</sup>, the  $a/d$  ratios for this study were continued from the starting point of 1.0. Girder A was tested once on each end, at  $a/d$  ratios of 2.5 and 2.0. Girder C was tested at  $a/d$  ratios of 3.0 and 3.83 (quarter point). The girders were supported at one end and at a location that left the opposite end overhanging such that it would not be damaged by or influence the test of the opposite end. Neoprene bearing pads were used to match field conditions. A single point load was applied through a steel plate using a hydraulic actuator. The applied force was measured using a 400-kip capacity load cell. Surface strain was measured at several locations during both tests. Deflection under the load point was measured using wire potentiometers and strand slip was monitored using LVDTs on selected strands at the tested end of the girders. A grid was drawn on the girders to assist in tracking the locations of cracks during testing. A 3 in. grid was used for girder A, while a 6 in. grid was used for girder C. Deflection of the bearing pads was monitored with two LVDTs on each end. Future work is forthcoming to elaborate on the results from much of the output, this paper will mainly focus on the failure mechanisms and ultimate loads achieved.

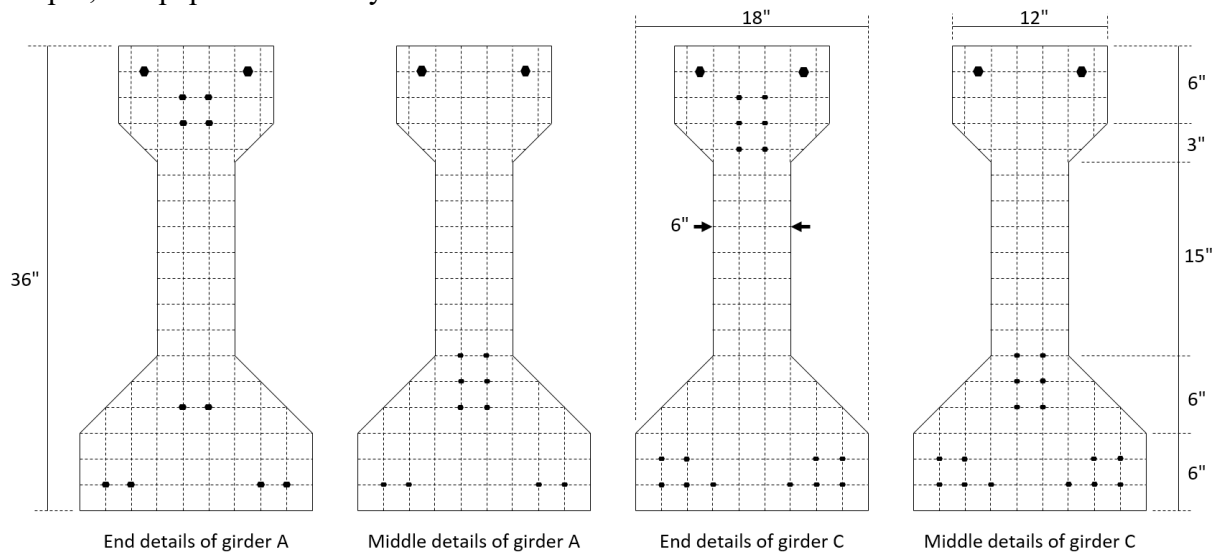


Figure 2: End and middle details of girders (2'' grid shown by dashed lines)

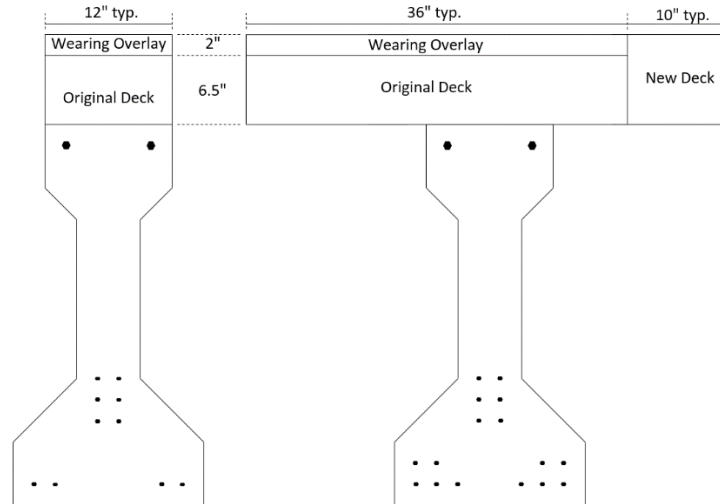


Figure 3: Details of remaining deck on girders A (left) and C (right)

In general, load was applied to the girders in 10-kip increments until initial cracking occurred; from this point on the load was applied in 5-kip increments. Cracks were marked as they occurred and load was increased incrementally until failure occurred. For all prediction methods, measured values of concrete strength were used as measured by cores taken from the girders.

## TESTING RESULTS

Flexural stiffness testing resulted in an average stiffness of  $388.2 \times 10^6$  kip-in<sup>2</sup> for girder A. This value was derived from the slope of the load deflection diagrams from the elastic flexural tests up to the applied force of 15 kips. Using the measured flexural stiffness and the calculated transformed section moment of inertia ( $104,949$  in<sup>4</sup>) implies a modulus of elasticity of 3700 ksi, which is 78% of the modulus of elasticity of cores taken from the girder (4750 ksi). These differences could be attributed to a number of factors including the difference in modulus of elasticity along the length of the girder, and inaccuracy of deflection measurements since the measured deflections were very small. Modulus was measured using individual cores taken from the center of the span and it is possible the modulus varies over the length of the girder which is not accurately represented by these discrete values. Deflection measurements using this method are very small compared to the size of the girder, therefore almost any error can influence the final result. The girder soffit was uneven, which resulted in variations in the support conditions some of which were of the same magnitude as the measured deflections. The deflections, including settlement at the supports, were measured with the best instruments available, however if this method is used in the future, care should be taken to eliminate sources of error in deflection measurement.

The cracking moments recorded also proved difficult to reconcile with the estimated prestress force. The cracking moments were taken during the shear tests of girder A, and as such there was some interaction of stresses due to moment, shear, and the draped strands.

The locations tested were also in or near discontinuity regions, where the “plane sections remain plane” assumption may not be accurate. Residual prestress forces calculated using the measured cracking moments from the test of each end were 97% and 105% of the initial prestress. By comparison, the expected prestress force based on AASHTO LRFD<sup>2</sup> was approximately 80% of the initial prestress.

A summary of all shear tests is shown in Table 1. The first shear test of girder A (A1) was performed at an  $a/d$  of 2.5 and a span length of 18.75 ft. Initial cracking occurred at a load of 170 kips directly under the load point. The first shear crack was a web shear crack 4.5 ft away from the load towards the near support and occurred at a load of 225 kips. As the load was increased, several shear cracks began to enter the bottom flange. At a load of 255 kips, the bottom four strands slipped, leading to a loss of load carrying capacity. Slip was measured for six of the strands before failure, possibly influenced by corrosion (Figure 4) present at the girder end. According to discussions with ODOT engineers, similar corrosion

Table 1: Summary of shear test information

<i>Test</i>	<i>a/d</i>	<i>Span (ft)</i>	<i>Failure load (kips)</i>	<i>Applied Shear (kips)</i>	<i>Failure mode</i>
<i>A1</i>	2.5	18.75	260	159	Bond-shear
<i>A2</i>	2.0	19	289.5	180	Flexural (strand rupture)
<i>C1</i>	3.0	25	318	204	Bond-Shear
<i>C2</i>	3.83	28	301	179	Compression-shear



Figure 4: Corrosion at tested end for A1

is frequently observed in Oklahoma bridges. Load was increased to 260 kips, at which point the deck overlay delaminated. The cracking pattern for this test is shown in Figure 5. This failure mode could be characterized as “bond-shear” because strand slip reduced the capacity of the section and ultimately led to failure. A picture of the failure is given in Figure 6.

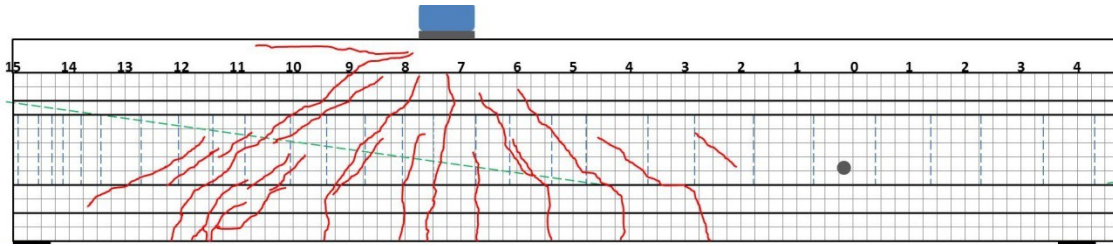


Figure 5: Shear test A1 cracking (3 in. grid shown)

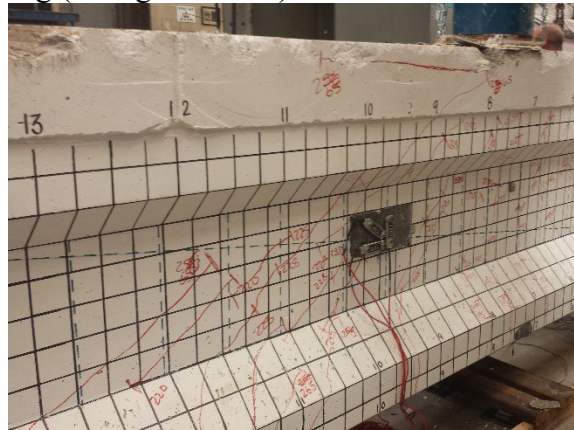


Figure 6: Shear test A1 failure, note deck overlay failure and shear cracking in the foreground

The second shear test of girder A (A2) was performed at an  $a/d$  of 2.0 and a span length of 19 ft. Initial cracking occurred at a load of 190 kips directly under the load point. The first shear crack was observed at a load of 225 kips in the web and the bottom flange roughly 1 ft away from the support. Load was increased to an ultimate capacity of 289.5 kips at which point there was a sudden failure corresponding to delamination of the deck overlay and rupture of multiple prestressing tendons. The strands ruptured roughly 1 ft away from the load point in the direction of the longer side of the span. The cracking pattern is shown in Figure 7 and a failure photo is given in Figure 8.

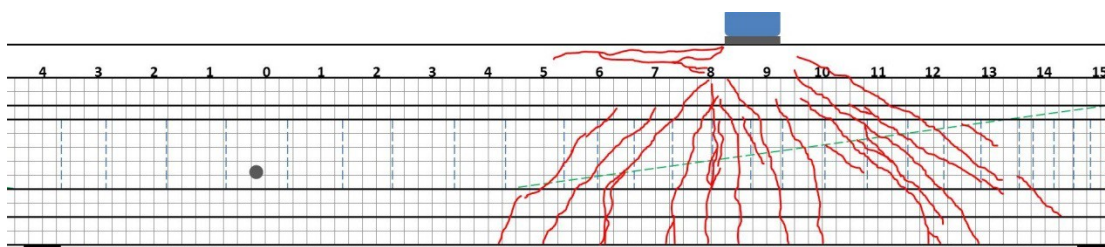


Figure 7: Shear test A2 cracking; strand rupture occurred at the 8-ft mark (3 in. grid shown)

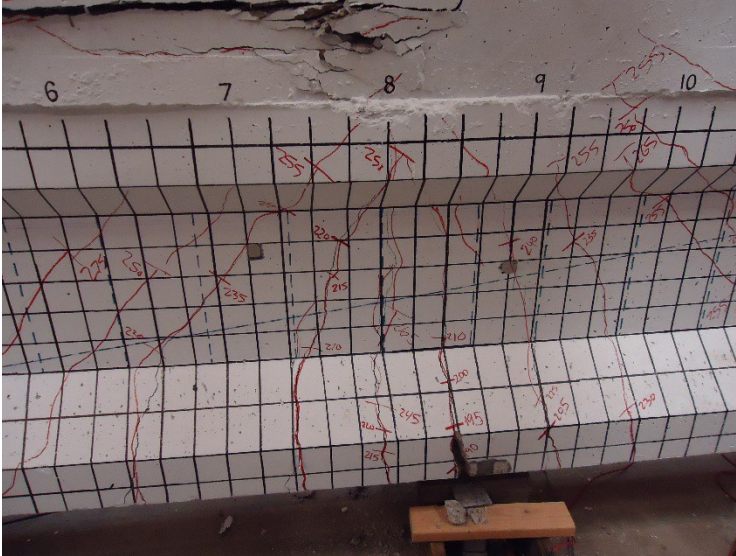


Figure 8: Test A2 failure, note deck crushing at the top of the image and the large flexural crack at the bottom where strand failure occurred

The first shear test of girder C (C1) was performed at an  $a/d$  of 3.0 with a span length of 25 ft. At an applied load of 90 kips, spalling was observed at the end nearest the load point. There was corrosion of the strands at that end similar to that described for girder A and the bearing force caused the pre-existing cracks caused by corrosion at this end to open and for pieces to spall off of the bottom flange (Figure 9). At this point the test had to be stopped so the LVDT's on the strands at that end could be repositioned. When the test was resumed, spalling more or less ceased and web-shear cracks were observed at a load of 160 kips at the web-top flange interface. Flexural cracking under the load was observed at 185 kips and at a load of 195 kips some shear cracks began to enter the bottom flange of the girder. A data acquisition error caused this test to be halted at 195 kips before continuing the load to failure. As load increased beyond 195 kips, several shear cracks began to align themselves with the strands in the bottom flange, indicative of a possible bond-shear issue. Once a load of 318 kips was reached, the shear cracks at the bottom flange became wider and the strands slipped leading to additional deflections and delamination and crushing of the deck overlay. The cracking pattern for test C1 is shown in Figure 10 and a photo of the failure is given in Figure 11.



Figure 9: Spalling under load initiated by cracking caused by corrosion

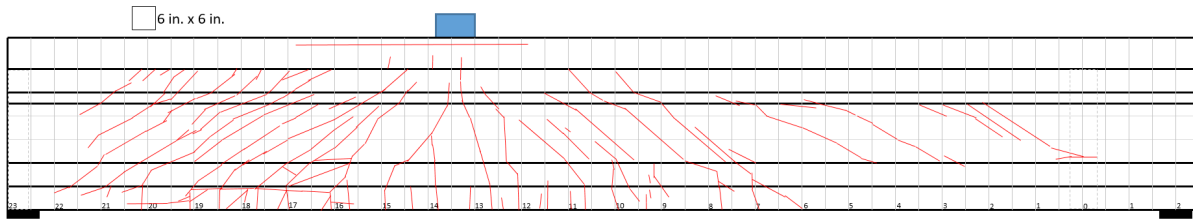


Figure 10: Test C1 cracking (6 in. grid shown)

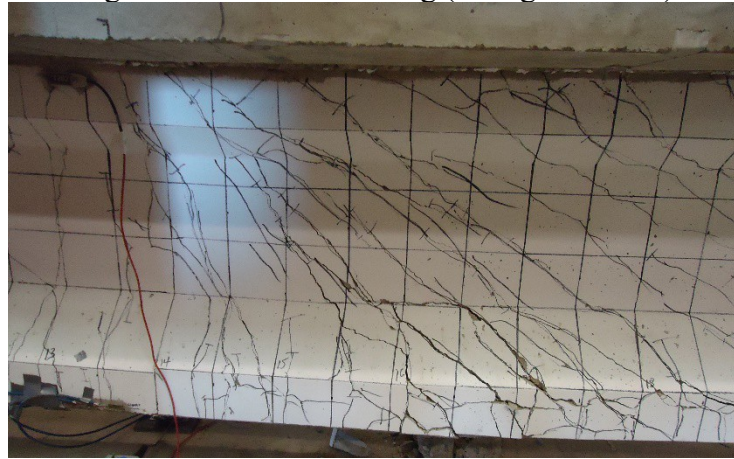


Figure 11: Test C1 failure, note large shear cracks and failure of the bottom flange concrete

The second test of girder C (C2) was performed at an  $a/d$  of 3.83, corresponding to a quarter of the original span length. In the 1973 AASHTO-STD this point would have been taken as the critical section for shear. However, this far into the span moment is expected to control the failure. The test span was increased to 28 ft to increase the shear demand on the short side of the span. The first observed cracks were web-shear cracks at a load of 150 kips followed by flexural cracking at 160 kips. At 195 kips of load, web-shear cracks entered the bottom flange of the girder. As in C1, some of these cracks oriented themselves in the direction of the strands as they entered the bottom flange. As in previous tests, the girder failed when the forces in the deck overlay were too large, causing the overlay to delaminate and crush. The max load was 301 kips. The compressive forces during this test were so large that the top flange crushed and compression steel in the top flange and the deck buckled. This failure type could be described as compression-shear or a flexural failure. Compression-shear is caused by shear cracks entering the compression flange<sup>21</sup>. The cracking pattern for test C2 is shown in Figure 12 and a photo of the failure is shown in Figure 13.

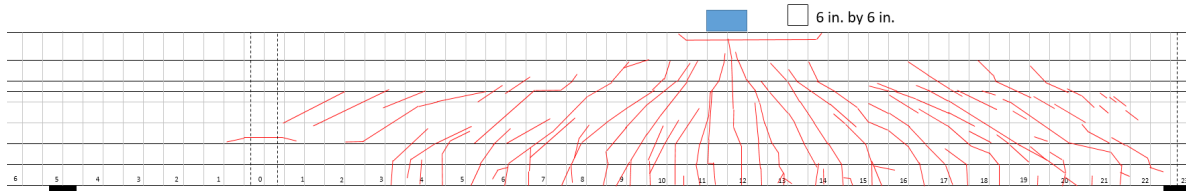


Figure 12: Test C2 cracking (6 in. grid shown)

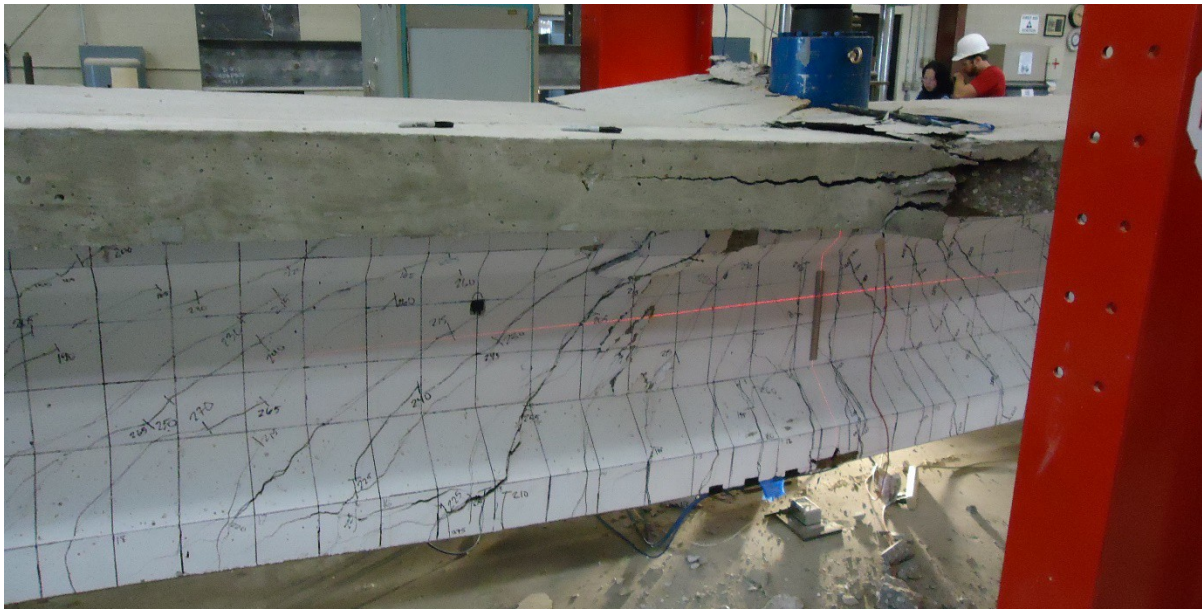


Figure 13: Test C2 failure, showing a large shear crack in the center of the image that entered the top flange causing catastrophic compression failure

#### COMPARISON OF TEST RESULTS TO CODES

Results from the four shear tests were compared to the ACI method (ACI), the 2012 AASHTO LRFD simplified procedure (2012-SIMP), the 2012 AASHTO LRFD general method (2012-GEN), the 1973 AASHTO Standard Specifications (1973-STD) and the AASHTO LRFD MCFT tabular method (2004-AASHTO). For this work,  $M_{max}$  was determined based on the expected flexural capacity of the section using strain compatibility.  $M_{cre}$  was determined using estimated effective prestress forces and including the dead load from the remaining deck. The code versus experimental capacities for all tests are shown in Figure 14. All expected capacities are nominal; no strength reduction factors are included in this paper.

In Figure 14 there is a general trend that the 2012-GEN and 2004-AASHTO methods (both based on MCFT) give conservative estimates of strength for each location tested. In the case of the 2012-GEN method, the estimate was conservative by a factor (predicted ultimate shear/experimental ultimate shear) of 0.40 to 0.56. The 2004-AASHTO methodology is slightly less conservative, with factors between 0.68 and 0.91. The 2012-GEN was developed

as a simplification of the 2004-AASHTO method and it was reported by its developers to be more conservative.<sup>12</sup> Both of these methods also predict a low concrete contribution to shear strength. The concrete contribution to shear strength is influenced by the factor  $\beta$  which differs between the 2004-AASHTO and 2012-GEN methods. In all cases, the 2012-GEN method provided a low capacity and predicted a large shear crack angle ( $\sim 50$  degrees), limiting the capacity from the stirrups. The equation for the shear crack angle is based on the strain at the level of the tension reinforcement; in these cases, the applied moment increased

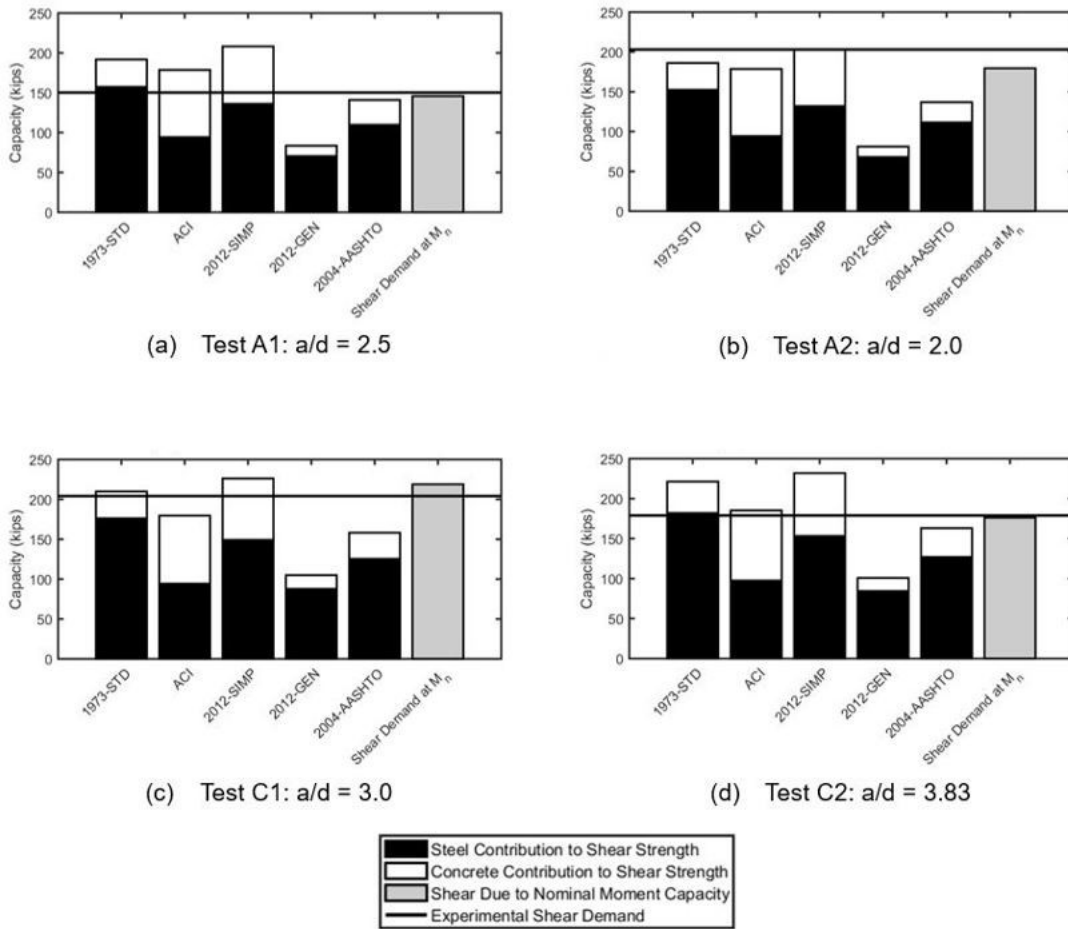


Figure 14: Tested capacities compared to codes

the strain, resulting in a reduced capacity. The moment was relatively high because the girder had to be supported near the center to facilitate testing both ends, increasing the applied moment for a given shear demand. The 2004-AASHTO method produced an accurate prediction of shear crack angles, only differing with the actual shear crack angle by an average of 3 degrees.

The other shear equations were occasionally un-conservative. For test A1, the 1973-STD, ACI, and 2012-SIMP were all un-conservative, over predicting capacity by factors of 1.20, 1.12, and 1.31 respectively. During test A1 there was a loss of bond due to shear cracking

and possibly due to corrosion. This test can be characterized as a bond-shear failure. Based on strain compatibility, the flexural capacity of the section should have been reached at an applied load of 239 kips; less than the 260 kip applied load at failure. In this case, the capacity of the section can be estimated conservatively by strain compatibility, even when bond is lost due to shear cracking. One could argue that the estimated force to fail the section was conservative based on moment capacity determined by strain compatibility, however the shear equations failed to predict a loss of bond due to shear cracking, which is potentially un-conservative. Future work will involve analysis using a free body diagram at the shear crack face to determine the expected capacity after the shear crack forms, similar to the method reported by Ross and Naji.<sup>25</sup>

During test A2, prestressing strands near the load point ruptured, indicating a flexural failure. The flexural capacity of the section based on strain compatibility was exceeded during the test. The extent of shear cracking indicates that the girder maintained adequate ductility and load carrying ability during the test. At the failure load, all shear capacity calculations were conservative.

Test C1 resulted in a bond-shear failure with shear cracks entering the zone of prestress transfer and reducing the capacity of the section. The codes were conservative with the exception of the 2012-SIMP (by a factor of 1.11). Test C2 on the other hand was performed at the quarter-point, the critical location for shear per the 1973 code. The span length was increased to 28 ft for this test to increase the shear demand at the testing location. The girder failed when the deck and top flange crushed, indicating either a flexural failure or shear-compression failure.<sup>21</sup> In this case, the applied load exceeded the flexural capacity as calculated by strain compatibility. The code equations were conservative with the exception of the 1973-STD and 2012-SIMP by factors of 1.24 and 1.30 respectively.

Calculated shear capacities were normalized by the actual shear capacity to compare the accuracy of the different methods. Not considering test A2, which can be characterized as a flexural failure, the normalized capacities were averaged to determine how accurate they were in general. The results of this analysis are shown in Table 2. The 2012-GEN method is by far the most conservative, followed by the 2004-AASHTO method. ACI and the 2004-AASHTO provided the most accurate results in this study. The 1973-STD and 2012-SIMP methods were generally un-conservative for these cases. It is important to note that although this paper compares observed capacities to predicted shear capacities, these failures may not be entirely due to shear. Future work will also involve characterizing the failures in a more detailed fashion and comparing to other capacity models, including those that take into account loss of bond.

Table 2: Normalized capacities from each method

<i>Method</i>	<i>Average Normalized Capacity</i>	<i>Coefficient of Variation</i>
<i>1973-STD</i>	1.16	9.83%
<i>ACI</i>	1.01	12.1%
<i>2012-SIMP</i>	1.24	8.93%

<i>2012-GEN</i>	0.533	5.01%
<i>2004-AASHTO</i>	0.857	8.44%

In all of the tests performed for this study, there was a relatively high applied moment in relation to the applied shear, as compared to if the full span were tested. Because the spans were typically supported near the original girder centerline, higher loads were needed to reach the shear capacities of the sections. This changes the shear behavior by altering the internal stresses in the section. MCFT accounts for this by altering the angle of cracking based on the strain in the section. If these sections were loaded in the field, there would be a larger applied shear and smaller moment for a given load near the supports. The most concerning load case was test A1 because the shear capacity was underestimated by ACI and the 2012-SIMP and shear cracking caused strand slip in the section.

## CONCLUSIONS

As has been reported in the literature, shear capacity calculations can vary dramatically. For the tests described in this paper there was little agreement between different methods. The girders that were tested showed good ductility and a large amount of cracking before failure. The 2012-SIMP method was not a conservative method to calculate shear capacity for the bridge girders tested, and this research would indicate that the 2004-AASHTO method is the best balance of accuracy and conservatism. In all cases however, the applied loads exceeded expected loads whether determined from shear capacity calculations, or flexural capacity by strain compatibility. Future work on this project will involve evaluating the rest of the results of these shear tests and constructing scale sections to study the effects of the composite section on shear capacity. Continued work will also involve more detailed characterization of failure types and comparison with other models such as strut-and-tie and bond shear capacity.

Based on this work, the Type-II AASHTO girders tested behaved well, showing good ductility and load carrying capacity despite being in service for 45 years. Corrosion at the ends did cause some issues, especially at high loads. Spalling was often initiated by the corrosion cracking at the ends, potentially leading to bond loss, and bridge owners should be aware of this mode of deterioration since it is very common in simply supported precast concrete girder bridges.

## REFERENCES

1. AASHTO, Standard Specifications for Highway Bridges, Washington, D.C.: AASHTO, 1973.
2. AASHTO, AASHTO LRFD Bridge Design Specifications, Washington, D.C.: AASHTO, 2012.
3. ACI Committee 318, Building Code Requirements for Structural Concrete (ACI 318-14) and Commentary, American Concrete Institute, 2014.

4. Kaufman, K.M. and Ramirez, J.A. "Re-evaluation of the ultimate shear behavior of high-strength concrete prestressed I-beams," *ACI Structural Journal*, vol. 85, no. 3, May 1988, pp. 295-303.
5. Nordby, G.M. and Venuti, W.J., "Fatigue and Static Tests of Steel Strand Prestressed Beams of Expanded Shale Concrete and Conventional Concrete," *ACI Journal Proceedings*, vol. 54, no. 8, August 1957, pp. 141-160.
6. MacGregor, J.G., Sozen, M.A. , and Sless, C., "Strength of prestressed concrete beams with web reinforcement," *ACI Journal Proceedings*, vol. 62, no. 12, December 1965, pp. 1503-1520.
7. MacGregor, J.G. and Hanson, J.M., "Proposed Changes in Shear Provisions for Reinforced and Prestressed Concrete Beams," *ACI Journal*, vol. 66, no. 4, April 1969, pp. 276-288.
8. Wight, J.K. and MacGregor, J.G., *Reinforced Concrete: Mechanics and Design*, Upper Saddle River, NJ: Pearson Education, Inc., 2012.
9. Collins, M.P., Mitchell, D., Adebar, P., and Vecchio, F.J., "A General Shear Design Method," *ACI Structural Journal*, vol. 93, no. 1, January 1996, pp. 36-45.
10. Vecchio, F.J., and Collins, M.P., "The Modified Compression-Field Theory for Reinforced Concrete Elements Subjected to Shear," *ACI Journal Proceedings*, vol. 83, no. 2, March 1986, pp. 219-231.
11. Hawkins, N.M., Kuchma, D.A., Mast, R.F., and Reineck, K.-H., "NCHRP 549: Simplified Shear Design of Concrete Members," Transportation Research Board, Washington, D.C., 2005.
12. Bentz, E.C., Vecchio, F.J., and Collins, M.P., "Simplified Modified Compression Field Theory for Calculating Shear Strength of Reinforced Concrete Elements," *ACI Structural Journal*, vol. 103, no. 4, July 2006, pp. 614-624,.
13. Nilson, A.H., Darwin, D., and Dolan, C.W., *Design of Concrete Structures*, New York, NY: McGraw-Hill, Inc., 2005.
14. Schlaich, J., Schafer, K. and Jennewein, M., "Toward a Consistent Design of Structural Concrete," *PCI Journal*, vol. 32, no. 3, May-June 1987, pp. 74-150.
15. Shenoy, C.V., and Frantz, G.C., "Structural Tests of 27-Year-Old Prestressed Concrete Bridge Beams," *PCI Journal*, vol. 36, no. 5 Sept.-Oct. 1991, pp. 80-90.
16. Halsey, T.J. and Miller, R., "Destructive Testing of Two Forty-Year-Old Prestressed Concrete Bridge Beams," *PCI Journal*, vol. 41, no. 5, 1996, pp. 84-93.
17. Pessiki, S., Kaczinski, M., and Wescott, R.H., "Evaluation of Effective Prestress Force in 28-Year-Old Prestressed Concrete Bridge Beams," *PCI Journal*, vol. 41, no. 6, 1996, pp. 78-89.
18. Czaderski, C. and Motavelli, M., "Determining the Remaining Tendon Force of a Large-Scale, 38-Year-Old Prestressed Concrete Bridge Girder," *PCI Journal* , vol. 51, no. 4, 2006, pp. 56-68.
19. Lundqvist, P. and Riigimaki, J., "Testing of five 30-year-old prestressed concrete beams," *PCI Journal*, vol. 55, no. 4, 2010, pp. 50-58.
20. Hamilton III, H.R., Llanos, G., and Ross, B.E., "Shear Performance of Existing Prestressed Concrete Bridge Girders," University of Florida Department of Civil &

Coastal Engineering, Gainesville, FL, 2009.

21. Ross, B.E., Ansley, M.H., and Hamilton III, H.R., "Load Testing of 30-Year-Old AASHTO Type III Highway Bridge Girders," *PCI Journal*, vol. 56, no. 4, 2011, pp. 152-163.
22. Osborn, G.P., Barr, P.J., Petty, D.A., Halling, M.W., and Brackus, T.R., "Residual prestress forces and shear capacity of salvaged prestressed concrete bridge girders," *Journal of Bridge Engineering*, vol. 17, no. 2, 2010, pp. 302-309.
23. Martin, R.D., Kang, T.H.-K., and Pei, J.-S., "Experimental and code analyses for shear design of AASHTO prestressed concrete girders," *PCI Journal*, vol 56, no. 1, 2011, pp. .
24. Cranor, B.N., *Analysis and Experimental Testing for Shear Behavior of an AASHTO Type II Girder in Service for Several Decades*, Norman, OK: The University of Oklahoma, 2015.
25. Ross, B.E. and Naji, B., "A model for nominal bond shear capacity of pretensioned concrete girders," in *TRB 2014 Annual Meeting*, 2013.